Earth-based radar data reveal extended deposits of the Moon's Orientale basin

Rebecca R. Ghent
Department of Geology, University of Toronto, 22 Russell Street, Toronto, Ontario M5S 3B1, Canada
Bruce A. Campbell
Center for Earth and Planetary Studies, Smithsonian Institution, MRC 315, Washington, D.C. 20013, USA
B. Ray Hawke
Hawai'i Institute of Geophysics and Planetology, University of Hawai'i, Honolulu, Hawaii 96822, USA
Donald B. Campbell
Department of Astronomy, Cornell University, Ithaca, New York 14853, USA

ABSTRACT

We present new Earth-based radar observations of ejecta associated with the lunar Orientale impact basin. We can distinguish (1) a block-poor ejecta facies composing a concentric halo of mantling material 10 m or greater in thickness that extends more than 1000 km from the basin center, and (2) a melt-rich deposit that forms a discontinuous but areally extensive stratigraphic marker across the southern highlands. The melt-rich component likely extends well into the South Pole–Aitken basin, a key target for future landed and sample return missions. The observation of these two ejecta facies and their distribution across the southern nearside yields new insight into the types and distribution of material contributed by large basin-forming impacts to the highlands megaregolith.

Keywords: Moon, impacts, regolith, radar, Orientale.

INTRODUCTION

Bolide impacts have profoundly shaped the geological histories of the terrestrial planets. At millimeter and smaller scales, micrometeorite impacts are the major surface weathering process on airless bodies. At regional to global scales, extended deposits of impact basins formed during the period of heavy bombardment more than 3.85 b.y. ago (Chapman et al., 2007) dominate the upper crustal structure of the Moon, Mercury, and portions of Mars. Basin-forming impacts redistribute a significant volume of material over the surface, and in some cases may excavate lower crustal rocks. Craters of intermediate scale (meters to tens of kilometers) slowly overturn and mix the outer crust on these bodies, and their overlapping ejecta create local and regional variability in the regolith vertical structure.

Here, we present new Earth-based radar observations of ejecta associated with the Orientale basin, likely the youngest large multiringed basin on the Moon. We assess the influence of Orientale ejecta on the southern highlands megaregolith using the new radar imagery and associated echo polarization characteristics. These data provide quantitative information on the physical properties of the upper several meters of regolith, including likely sites of human exploration and sample return.

BACKGROUND

Basins on the Moon largely created the regional topography, and their ejecta compose the megaregolith, a several-kilometer-thick layer of variably pulverized crustal material. The central regions of most nearside basins were later flooded by basaltic lava, but the intervening highlands retain a geologic record dating back to the formation of the giant South Pole–Aitken (SP-A) basin, which is more than 12 km deep at its center. Our focus here is the southern nearside highlands (Fig. 1), where a SP-A-derived basement is overlain by varying thicknesses of material from subsequent basins. At the western limb, the Orientale basin is delineated by at least four rings (Fig. 1A). Terrain within the inner ring (320 km in diameter; "ring 1") is partially filled by basaltic lava; the Inner Rook (d = 480 km; ring 2), Outer Rook (d = 620 km; ring 3), and Cordillera (d = 930 km; ring 4) rings are defined by massifs and quasi-circular mountain ranges. Previous geologic mapping, based on Lunar Orbiter photographs, delineated geological units based on surface morphology, spatial distribution, and population of superposed craters (Wilhelms et al., 1979). These authors defined the Imbrian-aged Hevelius Formation, with a thick, strongly lineated inner facies (Iohi), a discontinuous outer facies (Ioho) consisting of ejecta from secondary craters, and a smooth, nonlineated facies (Iohn) characterized by lobes suggesting fluid-like flow, perhaps from impact melt. An Imbrian-aged "light plains" unit (Ip) was mapped as gradational with all three Hevelius members, and characterized as a smooth, mantling ejecta deposit that occupies low areas. Wilhelms et al. (1979) also suggested that nearby fractured floor material (Ifc) could be Orientale-derived impact melt. Moore et al. (1974) and Howard and Wilshire (1975) documented evidence for extensive melt in exposed areas of the Orientale basin floor and limited areas exterior to the crater, including ponding, flow structures, fracturing of smooth deposits, and mantling of topography.

Previous regional studies relied on variations in surface geomorphology and small-crater population to associate various deposits with source basins. Complementary information on the physical properties of the upper 10 m or more of the regolith may be obtained from imaging radar observations, but until recently (Campbell et al., 2007a, 2007b) the coverage and resolution of such data have not been sufficient for detailed investigations of areas near the lunar limb. With the new observations presented here, we can examine the influence of Orientale ejecta on the southern highlands megaregolith.

METHOD

We use new Earth-based radar observations at 70 cm wavelength to examine regolith materials across the southern highlands, using the methodology described by Campbell et al. (2007a). We employ a bistatic observation system, transmitting circular-polarized radar signals from the Arecibo Observatory, and receiving reflected signals in both circular polarization states at the Green Bank Telescope. The received signals include reflections from the surface and, because the incident radar waves propagate into the regolith, reflections from subsurface rocks or rough

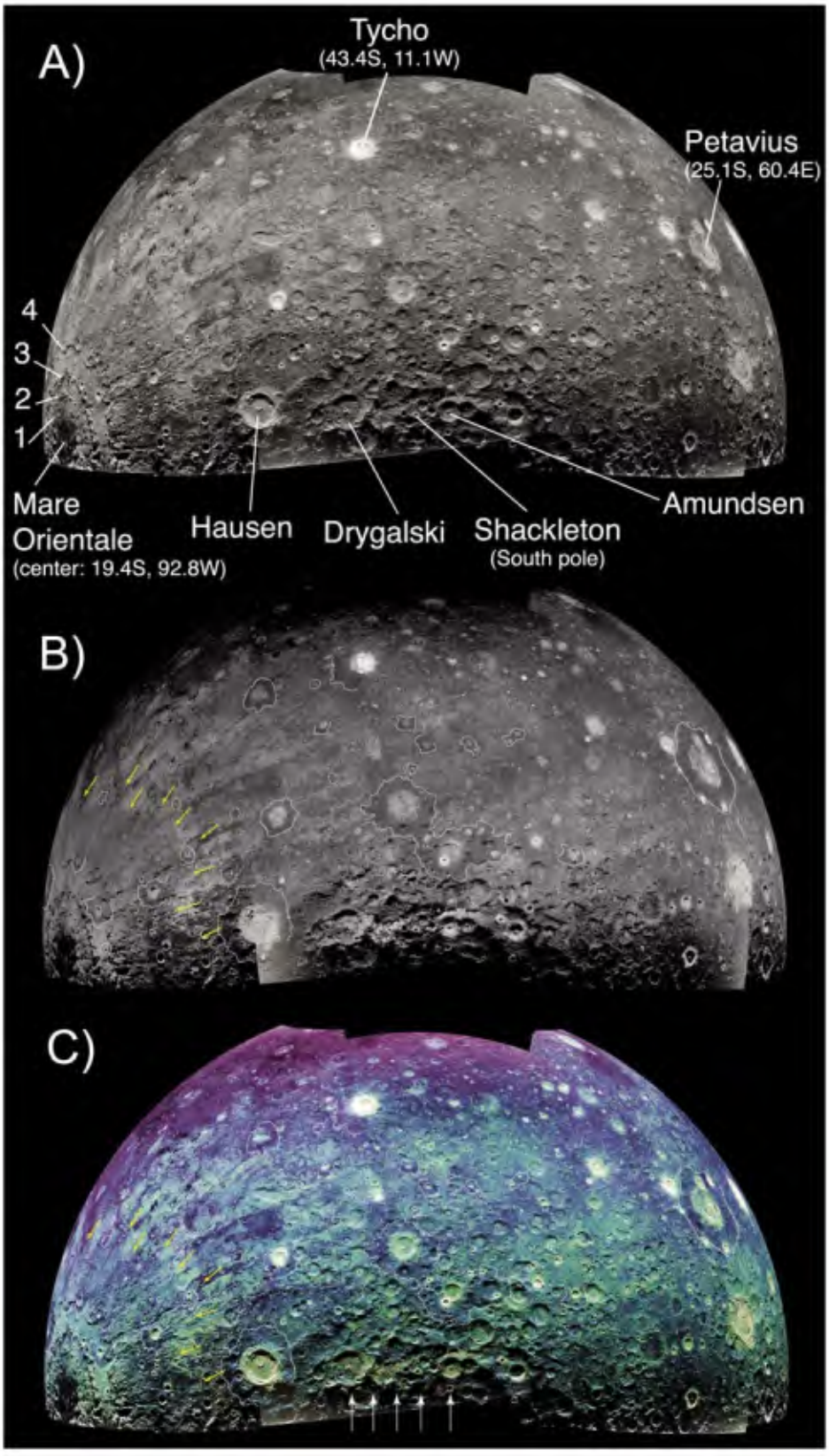

Figure 1. Seventy-centimeter radar mosaics for the southern nearside highlands; orthographic projection centered on the South Pole. A: SC mosaic; Orientale rings labeled 1 through 4. B: CPR mosaic. C: CPR mosaic (color) overlain on OC mosaic; white arrows indicate high-CPR "streak" that crosses the South Pole. Radar-dark crater haloes outlined; Orientale halo denoted by yellow arrows in B and C.

interfaces. Mirror-like (quasi-specular) reflections result in opposite-sense circular, or OC, reflections; diffuse scattering from wavelength-scale blocks on and within the regolith introduces reflections with the orthogonal polarization state, termed same-sense circular, or SC, reflections. Comparison of the calibrated echoes in the two channels yields information about the relative significance of specular versus diffuse scattering at any given location. In particular, the circular polarization ratio (CPR), or the ratio of SC to OC echoes, can be used to quantify the rock abundance at scales on the order of 10 cm and larger.

The penetration depth depends on the radar wavelength and the microwave loss properties of the target material. In highland regolith, the radar penetrates to depths of 10–20 times the illuminating wavelength (Campbell and Hawke, 2005). The observed echo thus represents the depth-integrated response of the regolith along the radar path length and can be used to constrain physical regolith properties in a corresponding volume of material.

RESULTS: RADAR PROPERTIES OF ORIENTALE BASIN MATERIAL

Orientale Block-Poor Ejecta

The 70 cm SC echoes (Fig. 1A) show strong variations associated with large-scale topography. Crater walls and other topographic scarps facing the incident radar energy act as specular reflectors, and thus appear bright, and young craters show bright annuli due to scattering from large blocks on/within their continuous ejecta blankets. Because the Moon is continually bombarded, large blocks are comminuted into smaller particles with time, so that older crater ejecta are not as bright in radar images as younger, blockier ejecta (Thompson et al., 1974). Since the CPR is sensitive to the population of wavelength-scale scatterers on or in the regolith, fresh crater ejecta also have high CPR values (Figs. 1B and 1C).

Many of the craters in Figure 1 show low 70 cm radar returns in annuli outside their bright, proximal ejecta, and these haloes are also apparent in the CPR mosaic (Fig. 1B). Such haloes are ubiquitous in association with nearside craters younger than the Early Imbrian epoch (Ghent et al., 2005), including the large craters Plato and Sinus Iridum (Thompson et al., 2006). The haloes comprise an ejecta facies, at least a few meters thick, that is depleted in surface and suspended scatterers ≥10 cm in diameter. Haloes of relatively low nighttime residual temperatures were also observed in data from the Apollo 17 Scanning Infrared Radiometer, consistent with depletion in blocks >30 cm in diameter (Schultz and Mendell, 1978). Preliminary new observations of young craters such as Aristarchus and Tycho at 12.6 cm wavelength also show haloes, indicating depletion of fragments ≥2 cm in

diameter. Radar-dark crater haloes are not present for older craters, because impact gardening homogenizes the block distribution of the halo area with the background terrain.

The ubiquity of radar-dark haloes in association with Imbrian-aged and younger craters suggests that the production of block-depleted ejecta is a process characteristic of all large lunar impacts. Consistent with this idea, an annulus of low radar return is associated with Orientale, beginning outside the Cordillera ring (ring 4; Figs. 1B and 1C). The annulus's digitate margins in some locations follow individual ridges and furrows in the Hevelius Formation, and cut across Hevelius lobes in others. Toward the south, the halo margin is difficult to delineate because of overlapping deposits from younger craters such as Hausen. We estimate the radius of the Orientale halo to be 1050 km.

Orientale Impact Melt Deposits

Regional variations in decimeter-scale block population are also revealed by the CPR data (Fig. 1C). Patches of enhanced CPR form a pattern roughly radial to Orientale, extending >2700 km from the basin center. This fabric shows moderately high SC echo strength (Fig. 1A) and high CPR values (Fig. 1B), suggesting that the streaks contain decimeter-scale blocky fragments on or within tens of meters of the surface. The patches are typically correlated with smooth materials in crater floors and other topographic depressions, and with smooth "ponds" in the rugged highlands. Many of these smooth deposits were mapped using photographs as Imbrian-aged light plains and were attributed by some workers to a fluid, perhaps melt-rich, component of basin ejecta (e.g., Eggleton and Schaber, 1972; Moore et al., 1974). The melt-rich explanation gained support with analysis of one high-CPR "streak" that crosses the South Pole (Fig. 1C, white arrows), where high-resolution images show abundant 100 m radar-bright craters that have apparently excavated a near-surface layer of competent material (Campbell and Campbell, 2006; Campbell et al., 2006).

With the regional view afforded by the new radar observations, we can now associate these isolated patches with the more extensive fabric of enhanced CPR across the southern highlands, and attribute this wider pattern to melt-rich ejecta from Orientale. Like the south polar streak, the other high-CPR patches are composed of a high density of kilometer-scale, very high-CPR points amid a more typical moderate-CPR background, again suggesting a near-surface source of locally coherent material. The average radar brightness and CPR decrease with increasing distance from Orientale, suggesting smaller volumes of melt. The smooth areas along the Drygalski-Shackleton-Amundsen line have higher CPR than patches elsewhere on the nearside, reflecting either an observational effect (the radar incidence angle is highest along the lower part of the radar image) or a fortuitous occurrence of more abundant melt within this lobe of Orientale ejecta. The high-CPR patches provide a time-stratigraphic marker across the region.

Some high-CPR patches are correlated with deposits previously mapped as Nectarian-aged light plains by Wilhelms et al. (1979), though those authors point out that because of uncertainties associated with crater statistics, some instances of the Nectarian unit "Ntp" could be younger or older. Association of these patches with Orientale ejecta suggests that some instances of Ntp could in fact be Imbrian in age. These areas could be targeted by the high-resolution Lunar Reconnaissance Orbiter Camera to address this question via refined crater counts.

IMPLICATIONS OF ORIENTALE DEPOSITS

Thompson et al. (2006) showed that for nearside craters ranging in size from Aristarchus (d = 40 km) to Sinus Iridum (d = 236 km), crater and radar-dark halo radii are related by the power-law function

$$t = kr_c^{0.74}\left(\frac{r_c}{r}\right)^3, \quad (1)$$

where k is an empirically determined constant, t is the ejecta thickness, r is the distance from the source crater, and r_c is the transient crater radius (McGetchin et al., 1973). Fine material represents an increasing fraction of the total ejecta volume with increasing distance from the crater. We can use Equation 1 to analyze radar-dark haloes if we apply it at the distal halo edges, where we assume that 100% of the ejecta volume consists of fine material. If the thickness of halo material at the distal margins is denoted as t_H, the relationship between crater and halo radii becomes

$$r_H = Ar_c^{1.25}, \quad (2)$$

where $A = (k/t_H)^{1/3}$, and t_H is the ejecta thickness at the halo margins (Thompson et al., 2006). We assume that t_H is uniform for all craters used in this study, because it corresponds to the minimum thickness of halo material required for detection using 70 cm radar imaging. Therefore, the value for A is likewise uniform; we find the best-fit value for A using the 16 craters shown in Figure 2. For large craters, the transient crater is generally smaller than the final crater, which is enlarged by postimpact slumping and other modification processes; here, we use the present-day crater radius as an approximation for r_c.

We now include Orientale in this analysis. Unlike the smaller craters, Orientale is a multi-ringed basin, with at least four possible values for transient crater radius (Spudis, 1993), corresponding to the rings shown in Figure 1A. The curve defined by Equation 2 falls closest to Orientale ring 2, but overpredicts the corresponding halo size (Fig. 2). Because current crater size is an upper bound on transient crater size, this result is consistent with the notion that the transient crater for Orientale lay between current rings 1 and 2, based on reconstructions of the transient cavity using the basin's gravitational and topographic signatures (Wieczorek and Phillips, 1999). Further, this result shows

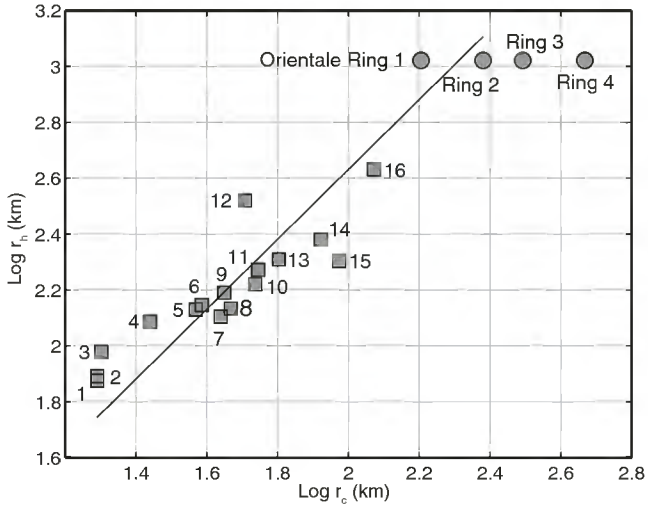

Figure 2. Log-log plot of halo radius versus crater radius for 16 large nearside craters. Trend represents fit to equation 2 in text ($r_H = 0.244r_c^{1.25}$; r_H and r_c in m) for numbered craters. Also shown are Orientale rings. Numbered craters: 1—Harpalus; 2—Autolycus; 3—Aristarchus; 4—Aristillus; 5—Stevinus; 6—La Pérouse; 7—Aristoteles; 8—Copernicus; 9—Schluter; 10—Plato; 11—Moretus; 12—Tycho; 13—Langrenus; 14—Hausen; 15—Petavius; 16—Sinus Iridum.

that production of an extensive, highly comminuted facies, depleted in 10 cm and larger rocks, occurs with similar scaling over a large range of crater diameters. This fine material can therefore contribute significantly to the physical characteristics of the regional regolith.

DISCUSSION

In addition to previously recognized continuous ejecta and proximal melt sheets and lobate flows, the Orientale impact contributed a significant volume of both highly comminuted and melt-rich ejecta to the southern highlands regolith far from the crater. The melt-rich ejecta extend >2700 km across the nearside, partially or completely filling many smaller craters, and constituting a stratigraphic horizon. If other basin-forming impacts produced similar products, it is likely that at any location in the southern highlands, melt-rich rocks represent a component of the overlapping ejecta deposits. This result refines earlier views of the significance of melt in large-crater ejecta, previously thought to be largely confined to the region immediately exterior to the rims (e.g., Cintala and Grieve, 1998). This finding has implications for future exploration of the south polar region and the SP-A basin, both likely targets for future landed and sample return missions. A key science goal of current lunar exploration efforts is to determine the age of the SP-A basin (Committee on the Scientific Context for Exploration of the Moon, 2007), because as the oldest multiringed basin, SP-A provides a vital anchor for global crater chronology curves. Analysis of SP-A impact melts will provide essential constraints on this age. Wilhelms et al. (1979) estimated the location of the center of the SP-A basin as 56°S, 180°W, and its diameter as 2500 km. Using this location, the center of SP-A is ~2300 km from the center of Orientale; assuming symmetric distribution of Orientale ejecta, the high-CPR material could extend several hundred kilometers into SP-A. Sampling of materials in the interior of SP-A would thus include melt-rich material from Orientale, either as blocks of competent material at the surface excavated by small impacts, or buried beneath thin layers of regolith. Furthermore, other southern basins within range of SP-A likely produced their own melt-rich horizons. This new insight into the distribution of impact melt could inform efforts to unravel the stratigraphy of materials within the SP-A basin.

ACKNOWLEDGMENTS

We thank W. Mendell, T. Thompson, and an anonymous reviewer for helpful comments. This work was supported by the National Aeronautics and Space Administration (NASA) Planetary Astronomy program and the NASA Planetary Geology and Geophysics program. Arecibo Observatory is part of the National Astronomy and Ionosphere Center, operated by Cornell University under a cooperative agreement with the National Science Foundation. The Green Bank Telescope is part of the National Radio Astronomy Observatory, a National Science Foundation facility operated under cooperative agreement by Associated Universities, Inc.

REFERENCES CITED

Campbell, B.A., and Campbell, D.B., 2006, Regolith properties in the south polar region of the Moon from 70-cm radar polarimetry: Icarus, v. 180, p. 1–7, doi: 10.1016/j.icarus.2005.08.018.

Campbell, B.A., and Hawke, B.R., 2005, Radar mapping of lunar cryptomaria east of Orientale basin: Journal of Geophysical Research, v. 110, E09002, doi: 10.1029/2005JE002425.

Campbell, B.A., Campbell, D.B., Margot, J.-L., Ghent, R.R., Nolan, M., Carter, L.M., and Stacy, N.J.S., 2007a, Looking below the Moon's surface with radar: Eos (Transactions, American Geophysical Union), v. 88, p. 13–18, doi: 10.1029/2007EO020002.

Campbell, B.A., Campbell, D.B., Margot, J.L., Ghent, R.R., Nolan, M., Chandler, J., Carter, L.M., and Stacy, N.J.S., 2007b, Focused 70-cm radar mapping of the Moon: IEEE Transactions on Geoscience and Remote Sensing, v. 45, p. 4032–4042, doi:10.1109/TGRS.2007.906582.

Campbell, D.B., Campbell, B.A., Carter, L.M., Margot, J.-L., and Stacy, N.J.S., 2006, No evidence for thick ice deposits at the lunar south pole: Nature, v. 443, p. 835–837, doi: 10.1038/nature05167.

Chapman, C.R., Cohen, B.A., and Grinspoon, D.H., 2007, What are the real constraints on the existence and magnitude of the late heavy bombardment?: Icarus, v. 189, p. 233–245, doi: 10.1016/j.icarus.2006.12.020.

Cintala, M.J., and Grieve, R.A.F., 1998, Scaling impact melting and crater dimensions: Implications for the lunar cratering record: Meteoritics and Planetary Science, v. 33, p. 889–912.

Committee on the Scientific Context for Exploration of the Moon, Space Studies Board, Division on Engineering and Physical Sciences, National Research Council of the National Academies, 2007, The scientific context for exploration of the Moon: Washington, D.C., National Academies Press, 119 p.

Eggleton, R.E., and Schaber, G.G., 1972, Cayley Formation interpreted as basin ejecta: Apollo 16 Preliminary Science Report NASA SP-315: Washington, D.C., National Aeronautics and Space Administration, p. 29–7.

Ghent, R.R., Leverington, D.W., Campbell, B.A., Hawke, B.R., and Campbell, D.B., 2005, Earth-based observations of radar-dark crater haloes on the Moon: Implications for regolith properties: Journal of Geophysical Research, v. 110, E02005, doi: 10.1029/2004JE002366.

Howard, K.A., and Wilshire, H.G., 1975, Flows of impact melt at lunar craters: U.S. Geological Survey Journal of Research, v. 3, no. 2, p. 237–251.

McGetchin, T.R., Settle, M., and Head, J.W., 1973, Radial thickness variation in impact crater ejecta: Implications for lunar basin deposits: Earth and Planetary Science Letters, v. 20, p. 226–236, doi: 10.1016/0012-821X(73)90162-3.

Moore, H.J., Hodges, C.A., and Scott, D.H., 1974, Multiringed basins—Illustrated by Orientale and associated features: 5th Lunar Science Conference, Houston, Texas, 18–22 March 1974, Proceedings Volume 1 (A75-39540 19-91): New York, Pergamon Press, Inc., p. 71-100.

Schultz, P.H., and Mendell, W., 1978, Orbital infrared observations of lunar craters and possible implications for impact ejecta emplacement: Proceedings of the 9th Lunar Planetary Science Conference, Houston, Texas, 13–17 March 1978, p. 2857–2883.

Spudis, P.D., 1993, The geology of multi-ring basins: Cambridge, UK, Cambridge University Press, 277 p.

Thompson, T.W., Masursky, H., Shorthill, R.W., Tyler, G.L., and Zisk, S.H., 1974, A comparison of infrared, radar and geologic mapping of lunar craters: The Moon, v. 10, p. 87–117, doi: 10.1007/BF00562019.

Thompson, T.W., Campbell, B.A., Ghent, R.R., Hawke, B.R., and Leverington, D.W., 2006, Radar probing of planetary regoliths: An example from the northern rim of Imbrium basin: Journal of Geophysical Research, v. 111, E06S14, doi: 10.1029/2005JE002566.

Wieczorek, M.A., and Phillips, R.J., 1999, Lunar multiring basins and the cratering process: Icarus, v. 139, p. 246–259, doi: 10.1006/icar.1999.6102.

Wilhelms, D.E., Howard, K.A., and Wilshire, H.G., 1979, Geologic map of the south side of the Moon: U.S. Geological Survey Miscellaneous Investigations Series Map I-1162, scale 1:5,000,000.

Manuscript received 14 August 2007
Revised manuscript received 1 January 2008
Manuscript accepted 8 January 2008

Printed in USA